

A Simultaneous Coupled Nonlinear Algorithm for the Analysis of Steel Frames with Flexible Joints Considering Joint Unloading

Ali Abolmaali^{1,*}, Tri Le¹ and Zachary Godswel²

¹Department of Civil Engineering, University of Texas at Arlington, Arlington, Texas 76019, USA

²The University of North Dakota, Grand Forks, ND, USA

(Received: 13 March 2008; Received revised form: 20 August 2008; Accepted: 12 December 2008)

Abstract: This paper presents a finite element plasticity-based computer algorithm to analyze steel frames with flexible joints under static proportional loading, unloading, and reverse loading. Each connection mechanism is modeled using a rotational spring element with two nodes of identical spatial coordinates and the same translational degrees of freedom and different rotational degrees of freedom for modeling the relative rotation of the beam and ends of the connection. Instead of using a classical coupled nonlinear algorithm for the connection element and member geometric stiffness, a unique solution method is introduced that simultaneously iterates to find the incremental connection element and member geometric stiffness of the structure through solving the nonlinear system equation. To model unloading and reverse loading at the joints between beams and columns, a three-parameter, kinematics hardening model for moment-rotation behavior is considered. For proof-of-concept, a one-story, one-bay frame with two connections is considered for parametric study. It is shown that different connection constitutive equation (moment-rotation characteristic) in a frame could cause moment reversal in some connection(s).

Key words: frame analysis, flexible joints, connection unloading, finite element, nonlinear algorithm, kinematic hardening models.

1. INTRODUCTION

In conventional frame analysis, connections between beams and columns are ordinarily treated as either perfectly rigid or pinned. Perfectly rigid connections can also be called moment connections, as they allow full transfer of moment from beam to column. Pinned connections are commonly referred to as shear connections and act as hinges. Shear connections allow the full transfer of shear and axial forces between beam and column, but they do not allow transfer of moment. In reality, beam-to-column connections are neither perfectly rigid nor perfectly pinned. They display a nonlinear behavior that lies somewhere between the idealized rigid and pinned conditions. Moreover,

beam-to-column connections are subjected to axial and shear forces, bending moment, and torsion (Lui and Chen 1987). Axial and shear effects are usually small in comparison to rotation caused by bending moment acting on the connection (Lui and Chen 1987). For practical purposes, the behavior of connections is usually quantified by the relationship between applied bending moment and rotational deformation.

The nonlinear moment-rotation behavior of the connections in between the perfectly rigid and perfectly pinned cases. Connections that exhibit a lower initial stiffness often approach a lower ultimate moment. The ultimate moment is reached when a connection component is fractured or excessively yielded.

*Corresponding author. Email address: abolmaali@uta.edu; Fax: +817-272-2630; Tel: +817-272-3877.
Editor: K.F. Chung.

Connections behave in a nonlinear fashion because of a number of factors such as material discontinuity of the connection assemblage, local yielding of connection components, stress concentration at bolt holes and fasteners, geometric changes under applied loads, and local plate buckling (Chen *et al.* 1996).

The moment-rotation behavior (M- θ) of steel connections is normally obtained by experimental testing of the connection. Several researchers have reported static M- θ test data of connections, among which Chen and Lui (1991) and Chen *et al.* (1996) are known for their comprehensive M- θ data base. Also, several cyclic M- θ connection behaviors known as hysteresis behaviors are reported in literature among which Popov and Bertero (1973), Astaneh *et al.* (1989), Tsai *et al.* (1995), Kukreti and Abolmaali (1999), and Abolmaali *et al.* (2003) are referenced in this paper. The realization of the effect of semi-rigid joints on the overall frame behavior can be traced back to 1930s. Baker (1931) and Rathbun (1936) first applied conventional slope deflection and moment distribution to semi-rigid frame analysis, respectively. Monforton and Wu (1963) were first to incorporate the effect of flexible joints into the matrix stiffness method. This was done by modifying the beam-column element stiffness matrix to incorporate the effect of semi-rigidity. Similar algorithms were also introduced by Livesley (1964) and Gere and Weaver (1965). In these algorithms a linear moment-rotation connection curve and a factor were used to modify the beam-column element stiffness matrix. The dynamic behavior of frames with flexible joints was studied by Lionberger and Weaver (1969), Suko and Adams (1971), and LeMessurier (1974) conducted investigations on semi-rigid frame analysis, considering axial and shear deformations. From 1974 to present, more than twenty matrix stiffness method-based semi-rigid static and dynamic frame analysis techniques are reported among which Nethercot (1986), Lui and Chen (1987), Goto and Chen (1987), and Poggi (1988), Rodrigues *et al.* (1998), Christopher and Bjorhovde (1998), Abolmaali (1999) and Kukreti and Abolmaali (2000) are noted.

Most of the aforementioned studies, and those not referenced in this paper, do not specifically address the effect of the connection unloading due to connection moment redistribution at different incremental load levels. In semi-rigid frames subjected to distributed loads, connections' stiffness decrease with increasing moment. At bifurcation, some connections unload as the result of buckling due to rotation reversal (Chen *et al.* 1996). During unloading the stiffness of each unloaded connection increases up to the initial stiffness, which consequently increases the frame stiffness and enables

it to withstand additional load beyond bifurcation. On the other hand, if the column of a frame is subjected to a concentrated load in absence of the member loads, none of the connections will unload until bifurcation. Upon bifurcation the connection's stiffness decreases and no unloading will take place, and the frame becomes unstable. Also, frames made of different types of connections with different moment-rotation characteristics could undergo unloading in some connections depending on the beam and column's flexural rigidities.

The aforementioned discussion verifies the complex and unknown behavior of semi-rigid frames, which necessitates a detailed analysis technique that considers connection unloading. Indeed, during unloading some connection may undergo reverse loading, the effect of which must be incorporated in the analysis. Thus, this paper presents a unique plasticity-based solution method that iterates to find the simultaneous incremental member and geometric stiffness of the structure subjected to loading, unloading, and reverse loading.

2. FINITE ELEMENT MODELING OF SEMI-RIGID FRAMES

Based on finite element procedures, a steel frame with flexible joints can be considered as an assembly of beam-column elements and dimensionless rotational spring elements. Linear displacement based finite element, yields to the solution of linear equations:

$$[k]\{\delta\} = \{F\} \quad (1)$$

Where $\{F\}$ is the force vector containing all loads applied to the degrees of freedom of the structure, $[K]$ is the global stiffness matrix, and $\{\delta\}$ is the global displacement matrix. Generally, in structural analysis the external loads applied to the structure and boundary conditions are known, and displacements are solved from Eqn 1.

2.1. Beam-Column Element Stiffness

The stiffness of a beam-column element (including P- δ effect) in global coordinates is:

$$[k] = [k_{ea}] + [k_{eb}] + [k_g] \quad (2)$$

where $[k_{ea}]$ is the element axial stiffness matrix, $[k_{eb}]$ is the element bending stiffness matrix, and $[k_g]$ is the geometric stiffness matrix. In the elements of each of the matrices presented in Equation 2 is found in most of the textbooks in matrix methods for structural analysis such as Sack (1994).

2.2. Connection Spring Element Stiffness

In this study, steel connections were modeled as dimensionless spring elements with the same translational but different rotational degrees of freedom to model the relative rotation of the beam and column end rotations as shown in Figure 1. Assigning the same translational degrees of freedom to the connection element nodes ensures the equal movement of the point of intersection between beam and column. The relative rotation of the spring element can be calculated as

$$\theta_r = \theta_1 - \theta_2 \tag{3}$$

Where θ_1 is the rotation at the beam end of the spring and θ_2 is the rotation at the column end of the spring. Rotational degrees of freedom between beam and column are governed by the spring stiffness. The behavior of the spring is quantified only by the relationship between applied moment and relative rotation. The spring tangent stiffness matrix is made compatible with the beam-column element by making it a matrix of 6x6 in size shown as:

$$[K_{spring}] = \begin{bmatrix} 0 & 0 & 0 & 0 & 0 & 0 \\ 0 & 0 & 0 & 0 & 0 & 0 \\ 0 & 0 & K & 0 & 0 & -K \\ 0 & 0 & 0 & 0 & 0 & 0 \\ 0 & 0 & 0 & 0 & 0 & 0 \\ 0 & 0 & -K & 0 & 0 & K \end{bmatrix} \tag{4}$$

where K is defined as the derivative with respect to relative rotation θ_r of the kinematic hardening equation, which models the connection’s loading, unloading, and reverse loading, as shown graphically in Figure 2:

$$M = R_{ki} \theta_r \left(\frac{1 - R_b / R_{ki}}{\{1 + [(1 - R_b / R_{ki}) \theta_r / \theta_0]^n\}^{1/n}} + \frac{R_b}{R_{ki}} \right) \tag{5}$$

where R_{ki} is the initial connection stiffness, R_b is the slope of the asymptotic line, n is a shape parameter, and θ_0 is the reference plastic rotation and is given by:

$$\theta_0 = \frac{M_u}{R_{ki}} \tag{6}$$

where M_u is the ultimate connection moment. The tangent stiffness of the connection for any value of rotation is given by:

$$K = \frac{dM}{d\theta_r} = AD + ABE^{(-1/n)} - ABC^n \theta_r^n E^{(n-1-2/n)} \tag{7}$$

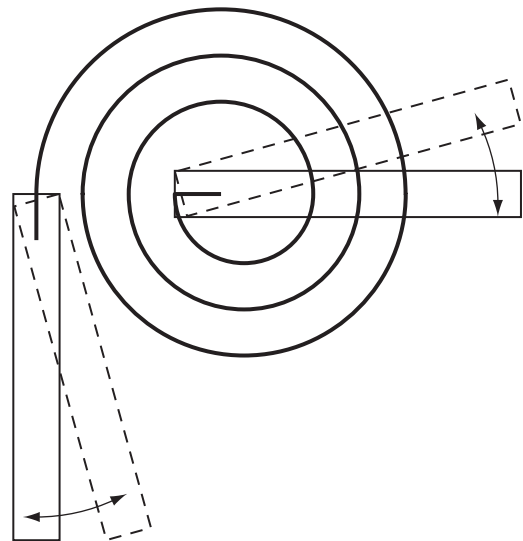


Figure 1. Graphical representation of connection spring element

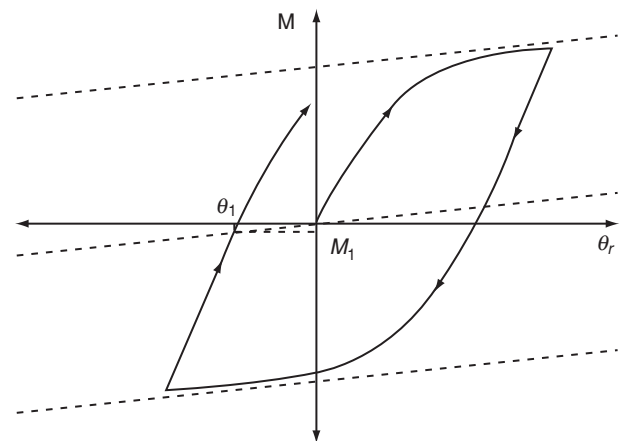


Figure 2. Kinematic hardening model for various values of n

where

$$A = R_{ki} \tag{8}$$

$$B = 1 - R_b / R_{ki} \tag{9}$$

$$C = B / \theta_0 \tag{10}$$

$$D = R_b / R_{ki} \tag{11}$$

$$E = 1 + C^n \theta_r^n \tag{12}$$

Finally, the effect of variation of the shape parameter, n , on the loading portion of the kinematic hardening equation is presented in Figure 3. This figure shows that by increasing the shape parameter, stiffer moment-rotation relations are obtained.

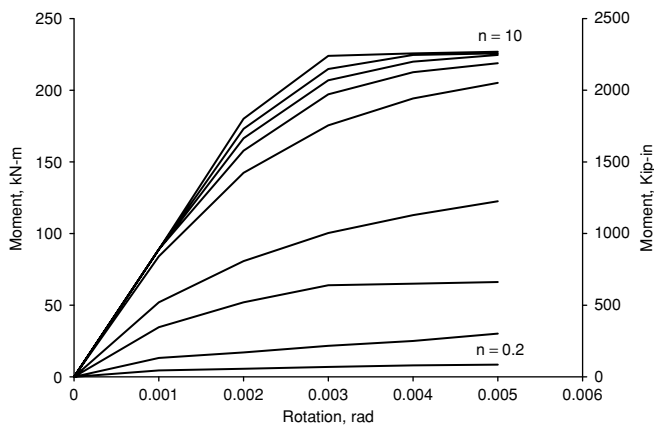


Figure 3. Effect of the shape parameter, n, on the loading portion of the kinematic hardening equation

3. NONLINEAR SOLUTION METHOD

This study employs a direct iteration method to solve the nonlinear system equation. The direct iteration method was used as an alternative to the classical Newton-Raphson method. In this method, the first load increment is solved using the initial stiffness, and in the subsequent load steps the stiffness of the connection is updated as follows:

$$k_{i+1} = \xi k_i + (1 - \xi) k_{is} \tag{13}$$

where

- k_{i+1} = stiffness for the next load increment
- ξ = descent parameter
- k_i = stiffness from the previous load increment
- k_{is} = secant stiffness from the previous load increment

The secant stiffness is calculated by finding the actual moment for the calculated rotation from the previous iteration solution. The descent parameter can be any number between 0 and 1, which if taken as 0 implies that the next iteration stiffness is the secant stiffness. Thus, the entries of the connection element stiffness matrix (Eqn 4) are updated to incorporate the change in the connection's stiffness. This is accomplished by replacing K_{33} , K_{36} , K_{63} , and K_{66} in Eqn 4 with the updated connection stiffness as calculated by Eqn 13. In the direct iteration method, instead of applying an unbalanced load to the structure to achieve convergence, a weighted effective stiffness is sought to satisfy the nonlinear system equation as shown in Figure 4. For the first iteration in a given load increment, the tangent stiffness is used. Thus, using the linear approximation of the first iteration, member displacements and forces are calculated and used to provide a better approximation of the effective stiffness across the incremental load step. For the connection element, the updated connection

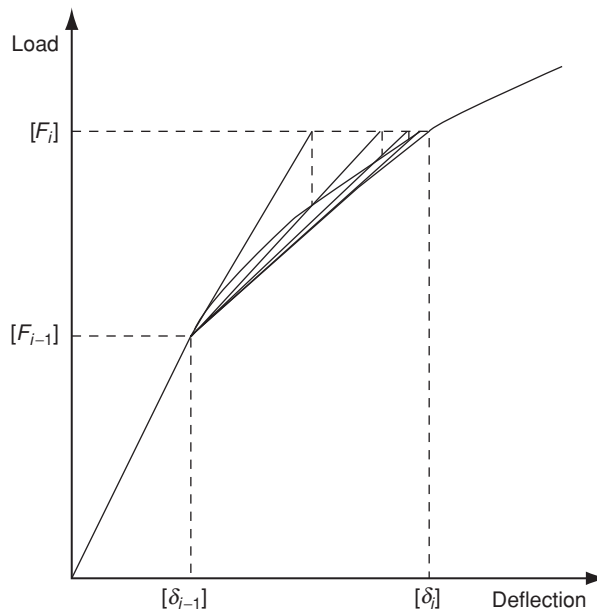


Figure 4. Direct iteration method of nonlinear analysis

stiffness is found by calculating the current iteration cycle secant modulus and obtaining a weighted average between it and the tangent modulus of the previous iteration. The actual connection moment for a given relative rotation is obtained by using Eqn 5 and dividing it by the relative rotation to find the secant stiffness in each iteration cycle.

For the beam-column, the stiffness for the next iteration cycle is obtained by substituting the geometric stiffness matrix from the elastic stiffness matrix using the axial force found for each member in the current iteration cycle. This is relatively simple for the first load increment. For subsequent load steps, however, incremental stiffness is not as simple to calculate.

Figure 5 represents the conceptual solution path for a single beam-column element, which is split up into two load increments. The first incremental solution is shown between the origin and point A. For the first load increment, a load of $\{f_1\}$ is applied to the element and the element undergoes a displacement $\{d_1\}$. The equation to be solved in the first load increment is:

$$\{f_1\} = ([k_e] - [k_{g1}])\{d_1\} \tag{14}$$

where $\{f_1\}_{6 \times 1}$ is the member force matrix for the first load increment, $[k_e]_{6 \times 6}$ is the sum of the axial and bending element stiffness matrices, $[k_{g1}]_{6 \times 6}$ is the geometric stiffness matrix for the first load increment (a function of axial force), and $\{d_1\}_{6 \times 1}$ is the displacement matrix for the element for the first increment of load. In Eqn 14, the sign convention for compressive member forces are taken to

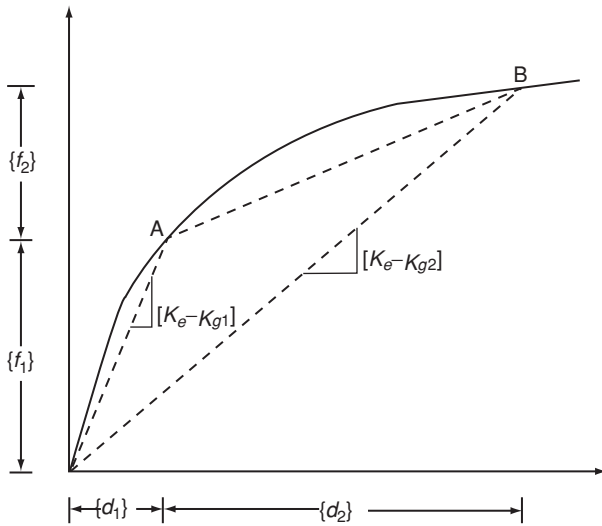


Figure 5. Conceptual representation of solution path for a beam-column element

be positive, which reduces member stiffness. Similarly, for the second incremental set of member forces $\{f_2\}$, the equation that applies to the situation is

$$\{f_1\} + \{f_2\} = ([k_e] - [k_{g2}])\{d_1\} + \{d_2\} \quad (15)$$

Where $\{f_2\}_{6 \times 1}$ is the incremental member force matrix for the second increment of load, $[k_{g2}]_{6 \times 6}$ is the geometric stiffness matrix for the total load after the second increment (a function of total axial load), and $\{d_2\}_{6 \times 1}$ is the incremental displacement matrix for the second load increment.

The previous equation reveals the problem of trying to apply the geometric stiffness matrix to an incremental solution method. It applies only to the total solution and not to the second increment of force alone. In order to apply an incremental solution, an equation of the following form is needed in order to apply the direct iteration method in terms of the second second set of incremental member forces:

$$\{f_2\} = [k_{effective}]\{d_2\} \quad (16)$$

To begin the process of putting together an equation of the form of Eqn 14, Eqns 11-12 can be rearranged as follows:

$$\{f_2\} = [k_e]\{d_2\} + [k_{g1}]\{d_1\} - [k_{g2}]\{d_1\} - [k_{g2}]\{d_2\} \quad (17)$$

The problem that becomes evident in Eqn 15 is that there is no apparent way to isolate the right side of the equation in terms of the second incremental

displacement $\{d_2\}$. However, Eqn 17 can be further manipulated as follows:

$$\{f_2\} = ([k_e] + ([k_{g1}] - [k_{g2}])\{d_1\}\{\alpha\} - [k_{g2}])\{d_2\} \quad (18)$$

where $\{\alpha\}$ can be defined as a 1×6 matrix subject to two conditions:

$$\{\alpha\}\{d_2\} = [1] \text{ (a } 1 \times 1 \text{ matrix)} \quad (19)$$

$$([k_{g1}] - [k_{g2}])\{d_1\}\{\alpha\} \quad (20)$$

= a square 6×6 symmetric matrix

The constraint in Eqn 19 is insufficient alone to solve for $\{\alpha\}$ because there are an infinite number of solutions to that equation. The symmetric constraint of Eqn 20 brings the number of solutions for $\{\alpha\}$ to exactly one. The reason that the symmetric constraint is valid is because the member stiffness matrix must be symmetric or the beam-column elements will not obey equilibrium. Subject to the given constraints, the $\{\alpha\}$ matrix is calculated as follows:

$$\alpha_6 = \frac{\phi_6}{\phi_1 d_{i(1)} + \phi_2 d_{i(2)} + \phi_3 d_{i(3)} + \phi_4 d_{i(4)} + \phi_5 d_{i(5)} + \phi_6 d_{i(6)}} \quad (21)$$

$$\alpha_5 = \frac{\phi_5 (1 - \alpha_6 d_{i(6)})}{\phi_1 d_{i(1)} + \phi_2 d_{i(2)} + \phi_3 d_{i(3)} + \phi_4 d_{i(4)} + \phi_5 d_{i(5)}} \quad (22)$$

$$\alpha_4 = \frac{\phi_4 (1 - \alpha_6 d_{i(6)} - \alpha_5 d_{i(5)})}{\phi_1 d_{i(1)} + \phi_2 d_{i(2)} + \phi_3 d_{i(3)} + \phi_4 d_{i(4)}} \quad (23)$$

$$\alpha_3 = \frac{\phi_3 (1 - \alpha_6 d_{i(6)} - \alpha_5 d_{i(5)} - \alpha_4 d_{i(4)})}{\phi_1 d_{i(1)} + \phi_2 d_{i(2)} + \phi_3 d_{i(3)}} \quad (24)$$

$$\alpha_2 = \frac{\phi_2 (1 - \alpha_6 d_{i(6)} - \alpha_5 d_{i(5)} - \alpha_4 d_{i(4)} - \alpha_3 d_{i(3)})}{\phi_1 d_{i(1)} + \phi_2 d_{i(2)}} \quad (25)$$

$$\alpha_1 = \frac{(1 - \alpha_6 d_{i(6)} - \alpha_5 d_{i(5)} - \alpha_4 d_{i(4)} - \alpha_3 d_{i(3)} - \alpha_2 d_{i(2)})}{d_{i(1)}} \quad (26)$$

where

$$\{\phi\}_{6 \times 1} = ([k_{g2}] - [k_{g1}])\{d_{i-1}\} \quad (27)$$

and $\{d_{i-1}\}_{6 \times 1}$ is the total displacement vector at the end of the previous load increment ($\{d_1\}$ in the given example with two load increments), and $\{d_i\}_{6 \times 1}$ is the member displacement matrix for the current load increment.

With $\{\alpha\}$ known, the effective stiffness for a given increment of load to be used in the direct iteration formulation is as follows:

$$[k_{effective}] = [k_e] + ([k_{g1}] - [k_{g2}])\{d_1\}\{\alpha\} - [k_{g2}] \quad (28)$$

4. PROGRAM ALGORITHM

The frame analysis program that is presented in this paper considers the unloading connection behavior, the P-Δ effect, and nonlinear connection behavior according to the kinematic hardening equation. For ease of reading, the step-by-step procedure for the first load step will be summarized first in which unloading is not considered. After the first load step, the algorithm for an arbitrary load step is then presented.

4.1. Program Algorithm for the First Load Increment

1. Assemble the elastic stiffness matrix $[K_e]$ for each frame element. Formulate the initial tangent stiffness matrix for each connection element. Assemble the system global stiffness matrix, $[K]$, for the entire frame using conventional methods.
2. Assemble the system load vector, $\{F\}$. Distributed loads are converted to equivalent nodal loads. These equivalent loads will be copied to another matrix containing fictitious end forces so that they can be removed when local member end forces are calculated.
3. Divide the load vector by the number of load steps to be applied to the frame. This is the incremental load vector that will be applied at each load step.
4. Using the assembled initial tangent stiffness matrix, the incremental system equilibrium equation is solved for nodal displacements, $\{\delta\}$.
5. For each frame element, member forces are calculated in the local coordinate system and axial forces are identified.
6. The axial force calculated from Step 5 is used to calculate geometric stiffness matrix. For the next iteration of this load step, the frame element stiffness will be as follows:
7. $[k] = [k_e] + [k_g]$ (29)
8. For each spring element, relative rotation is as follows:

$$\theta_r = \theta_1 - \theta_2 \quad (30)$$

where θ_1 and θ_2 are the rotations at each node of the spring element. The sign of θ_r depends on the order in which the spring element nodes were inputted into the program and has no effect on the results of the analysis.

9. The actual connection moment for the given relative rotation is calculated using:

$$M_{act} = \left[\theta_r R_{ki} \left(\frac{1 - R_b / R_{ki}}{\{1 + [(1 - R_b / R_{ki})\theta_r / \theta_0]^n\}^{1/n}} + \frac{R_b}{R_{ki}} \right) \right] \quad (31)$$

10. The secant stiffness (calculated using Eqn 13) is substituted into the connection stiffness matrix. It should be noted that the descent parameter was set at zero for this analysis.

$$k_{33} = \frac{M_{act}}{\theta_r} \quad (32)$$

$$k_{36} = -\frac{M_{act}}{\theta_r} \quad (33)$$

$$k_{63} = -\frac{M_{act}}{\theta_r} \quad (34)$$

$$k_{66} = \frac{M_{act}}{\theta_r} \quad (35)$$

11. The global stiffness matrix is assembled with the updated frame and connection element stiffness matrices. The incremental equilibrium equation with the updated system stiffness is solved. Steps 5 through 11 are solved until a convergent solution for the first load step is obtained.

4.2. Program Algorithm for an Arbitrary Load Increment

1. The tangent stiffness of the structure is assembled for the first iteration of the current load step. For frame elements, the secant stiffness from the previous load step is an adequate approximation of tangent stiffness for the current load step. For spring elements, the following equation is now used to calculate the tangent stiffness of the spring element:

$$K = \frac{dM}{d\theta_r} = AD + ABE^{(-1/n)} - ABC^n \left(|\theta_r - \theta_1| \right)^n E^{(n-1-2/n)} \quad (36)$$

where θ_1 is the relative rotation at which the $M-\theta_r$ curve begins. It will be zero if no unloading occurs. See Figure 2.

2. The incremental system equilibrium equation is solved for nodal displacements.
3. The geomtric stiffness matrix for the total (not incremental) axial force for each frame element is calculated. Use the procedure outlined in Section 4 to determine the incremental stiffness for the given axial force in each member. This incremental secant stiffness will be the geometric matrix used in the next iteration for the current load step.
4. Determine the total relative rotation for each spring element. If the spring is not unloading, the actual incremental bending moment for the given relative rotation is calculated as follows:
For $\theta_r > \theta_1$,

$$M_{act} = \left| (\theta_r - \theta_1) R_{ki} \left(\frac{1 - R_b / R_{ki}}{1 + [(1 - R_b / R_{ki})(\theta_r - \theta_1) / \theta_0]^n} + \frac{R_b}{R_{ki}} \right) + M_1 - M_{prev} \right| \quad (37)$$

For $\theta_r < \theta_1$,

$$M_{act} = \left| (-\theta_r - \theta_1) R_{ki} \left(\frac{1 - R_b / R_{ki}}{1 + [(1 - R_b / R_{ki})(-\theta_r - \theta_1) / \theta_0]^n} + \frac{R_b}{R_{ki}} \right) + M_1 - M_{prev} \right| \quad (38)$$

where M_1 is the bending moment at which the $M-\theta_r$ curve begins, and M_{prev} is the total bending moment in the connection at the end of the previous load step. M_1 will be zero if no unloading occurs (refer to Figure 2).

5. Substitute the secant stiffness into the connection stiffness as follows:

$$k_{33} = \frac{M_{act}}{\theta_r - \theta_{r-prev}} \quad (39)$$

$$k_{36} = -\frac{M_{act}}{\theta_r - \theta_{r-prev}} \quad (40)$$

$$k_{63} = -\frac{M_{act}}{\theta_r - \theta_{r-prev}} \quad (41)$$

$$k_{66} = \frac{M_{act}}{\theta_r - \theta_{r-prev}} \quad (42)$$

where θ_{r-prev} is the total rotation at the end of the previous load step.

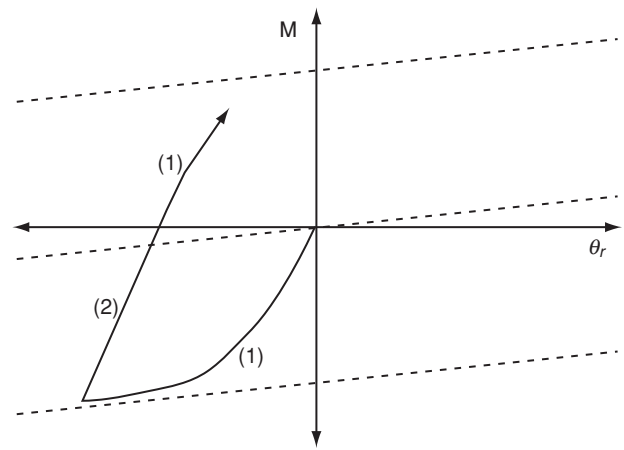


Figure 6. Graphical representation of two states of loading for springs

6. At each iteration of the current load step, check for unloading by determining which of the situations shown in Figure 6 applies to the state of spring loading.

Condition (1) occurs when the spring is loading with the kinematic hardening curve. Condition (2) corresponds to the state of a spring unloading and is modeled by a straight line with slope equal to the initial stiffness.

Load Condition (1):

$$\frac{K_{spring} (\theta_r - \theta_{r-prev}) + M_{prev} - M_1}{M_{max} - M_1} > 1 \quad (43)$$

Load Condition (2):

$$\frac{\theta_r R_b - M_1}{M_{max} - M_1} \leq \frac{K_{spring} (\theta_r - \theta_{r-prev}) + M_{prev} - M_1}{M_{max} - M_1} \quad (44)$$

where, M_{max} is the maximum difference between M_{prev} and M_1 at the end of the previous load step. M_{max} is set equal to M_1 when there is a transition from condition (2) to (1).

7. If the spring element unloads (meaning that condition 2 applies), substitute the following for the spring connection stiffness matrix:

$$k_{33} = R_{ki} \quad (45)$$

$$k_{36} = -R_{ki} \quad (46)$$

$$k_{63} = -R_{ki} \quad (47)$$

$$k_{66} = R_{ki} \quad (48)$$

8. The global stiffness matrix with the updated frame and spring element stiffness matrices are assembled.
9. The incremental equilibrium equation with the updated global stiffness is solved. Repeat steps 3-9 until the solution converges for the current load step.

5. VERIFICATION OF FRAME ANALYSIS PROGRAM

In order to verify the results obtained from the present study, two example problems were chosen from King and Chen (1993) and Bhatti and Hingtgen (1995) in which only the connection loading were considered in their semi-rigid frame analysis. For the aforementioned examples no moment reversal was possible; thus, it seemed logical to verify the computer program developed in this study with the results reported by King and Chen (1993) and Bhatti and Hingtgen (1995). The first example is a two-story one-bay frame, and the second example is a four-story two-bay frame, which are shown in Figures 14 and 15 respectively. For all analyses, E was taken as 200GN/m^2 (29000 ksi).

Example frame 1:

Bhatti and Hingtgen (1995) studied the frame of Example 1 (Refer to Figure 14) by using a bilinear model to describe the $M-\theta_r$ behavior of their connections. Thus, a high value of the rigidity parameter, n , was chosen in the kinematic hardening of Eqn 5 to approximate the $M-\theta_r$ model by Bhatti and Hingtgen (1995). The following values were used in the kinematic hardening spring element model:

$$R_{ki} = 88,892 \text{ kN-m/rad (786732 kip-in/rad)}$$

$$R_b = 0$$

$$\theta_0 = 0.00252818 \text{ rad}$$

$$n = 100$$

The analysis results for Example 1 are summarized in Tables 1 and 2 for maximum bending moments and lateral displacements, respectively. These tables show remarkable agreement between the present study and those reported by Bhatti and Hingtgen (1995). It seems that the kinematic hardening model was an adequate approximation of Bhatti and Hingtgen's (1995) bilinear connection behavior when appropriate parameters are employed.

Example frame 2:

Example 2 is a four-story, two-bay frame (refer to Figure 15) that was studied by King and Chen (1993).

$$R_{ki} = 88,892 \text{ kN-m/rad (786,732 kip-in/rad)}$$

$$R_b = 0$$

$$\theta_0 = 0.0035 \text{ rad}$$

$$n = 0.86$$

The analysis results for Example frame 2 are summarized in Tables 3 and 4 for maximum bending moments and lateral displacements, respectively. The results of the present study showed general agreement with those reported by King and Chen (1993) for the cases with rigid connections. There are slight variations in the results of flexible connections, which are attributed to the slight difference in the connection's moment-rotation behavior relation between the two studies. The connection behavior assumed in the present study was slightly less stiff than King and Chen's (King and Chen 1993) model over the range of bending moment taken by most of the connections. The higher drift values for the present study are attributed to the lower stiffness found in this range of the assumed $M-\theta_r$ behavior. For the most part, the present study agreed reasonably well with those reported by King and Chen (1993).

6. UNLOADING OF CONNECTIONS UNDER STATIC PROPORTIONAL LOADING

A parametric-type study was conducted on a simple one-story, one-bay frame with two connections as shown in Figure 7 to identify the unloading behavior of one of the frame's connection by varying the value of stiffness of the other connection. The connections on the left and right sides of the frame are designated as Connection 1 and Connection 2, respectively. The moment-rotation characteristics of each spring are assumed to be linear elastic. To investigate the behavior of the frame, the stiffness of Connection 1 was held constant at the value of 11,299 kN-m/rad (100,000 kip-in/rad), and the stiffness of Connection 2 was varied between 0 and 22,599 kN-m/rad (200,000 kip-in/rad). Figure 8 shows the results of this analysis. As the stiffness of Connection 2 increases beyond about 2,768 kN-m/rad (24,500 kip-in/rad), the sign of the moment across Connection 1 reverses.

The results of this study show that unloading can occur when a high degree of nonlinearity exists in the connections such that for a certain combination of gravity and wind loads (or anti-symmetric loading) the stiffness of one connection would degrade faster than the other connection, and consequently causes unloading in the connection with slower degradation rate. Moreover, if the two different kinds of connections with different stiffness degradation rates (different $M-\theta$ curves) are used in the aforementioned frame, then one of the connections will unload even though the applied load is anti-symmetric. For this example, the sign of the incremental moment taken by Connection 1 can be predicted using Figure 8,

Table 1. Absolute maximum bending moments kN-m (kip-in) for Example 1

Element No.	Rigid Connections		Rigid Connections with P-Δ		Flexible Connections with P-Δ	
	No P-Δ					
	Present Study		Present Study	Bhatti & Hingtgen	Present Study	Bhatti & Hingtgen
1	163 (1443)		189 (1677)	189 (1677)	196 (1739)	196 (1739)
3	80 (711)		90 (794)	90 (794)	102 (901)	102 (902)
5	80 (711)		90 (795)	90 (795)	102 (902)	102 (902)
6	163 (1450)		187 (1656)	187 (1654)	185 (1636)	185 (1634)
8	80 (711)		90 (795)	90 (795)	102 (902)	102 (902)
10	162 (1437)		189 (1669)	189 (1669)	196 (1732)	196 (1731)

Table 2. Lateral displacements m (in.) for Example 1

Node No.	Rigid Connections		Rigid Connections with P-Δ		Flexible Connections with P-Δ	
	No P-Δ					
	Present Study		Present Study	Bhatti & Hingtgen	Present Study	Bhatti & Hingtgen
2	0.02567 (1.011)		0.02966 (1.168)	0.02966 (1.168)	0.03752 (1.477)	0.03752 (1.477)
4	0.03883 (1.509)		0.04397 (1.731)	0.04397 (1.731)	0.0582 (2.292)	0.0582 (2.292)

Table 3. Absolute maximum bending moments kN-m (kip-in) for Example 2

Element No.	Rigid Connections with P-Δ		Flexible Connections with P-Δ	
	Present Study	King & Chen	Present Study	King & Chen
1	60 (534)	60 (534)	98 (867)	95 (843)
20	108 (957)	108 (957)	134 (1188)	132 (1170)
36	136 (1202)	136 (1202)	160 (1415)	158 (1397)
3	51 (455)	51 (455)	28 (244)	33 (291)
17	74 (657)	74 (656)	71 (629)	67 (596)
34	125 (1102)	124 (1101)	114 (1010)	118 (1044)
5	69 (615)	69 (615)	60 (529)	63 (559)
14	53 (473)	53 (473)	62 (547)	61 (542)
32	116 (1029)	116 (1029)	109 (964)	113 (996)
7	79 (703)	79 (702)	77 (684)	80 (705)
11	23 (200)	23 (200)	37 (324)	35 (313)
30	92 (818)	92 (818)	95 (838)	96 (846)

Table 4. Lateral displacements m (in.) for Example 2

Element No.	Rigid Connections with P-Δ		Flexible Connections with P-Δ	
	Present Study	King & Chen	Present Study	King & Chen
2	0.0068 (0.27)	0.0068 (0.27)	0.0103 (0.408)	0.0102 (0.40)
4	0.0168 (0.66)	0.0168 (0.66)	0.0282 (1.11)	0.0272 (1.07)
6	0.0238 (0.94)	0.0238 (0.94)	0.0424 (1.67)	0.0409 (1.61)
8	0.0282 (1.11)	0.0282 (1.11)	0.0516 (2.03)	0.0495 (1.95)

which indicates Connection 1 should begin to unload just as the value of tangential stiffness of Connection 2 drops below 2,768 kN-m/rad (24,500 kip-in/rad); otherwise, Connection 1 would not unload.

To further test the effect that the stiffness of Connection 2 has on the sign of moment taken by

Connection 1, a few changes were made to the connection behavior for the previous example to represent the real nonlinear M-θ behavior of a semi-rigid connection including directional anisotropy (kinematic hardening). The following values were used for the parameters of the kinematic hardening

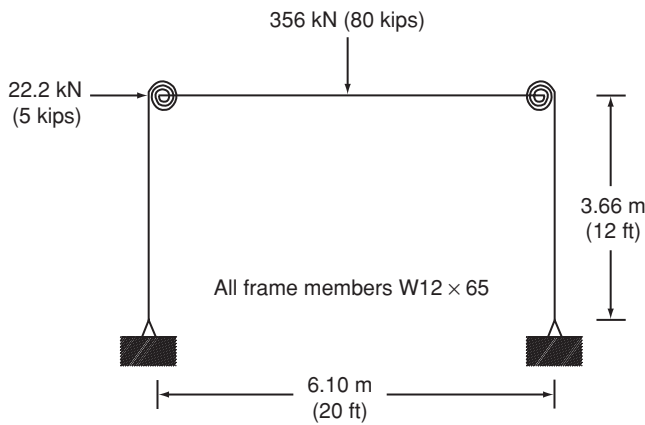


Figure 7. Simple one-story example used to show unloading behavior

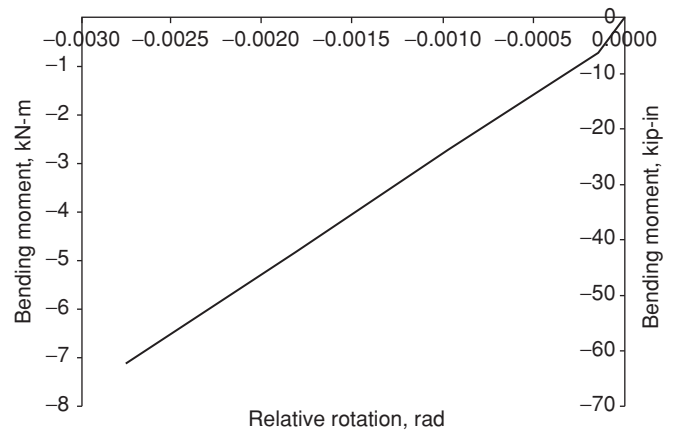


Figure 9. Moment-rotation behavior of connection 1 for connection 2 asymptotic stiffness of 3,420 kN-m/rad (30,000 kip-in/rad)

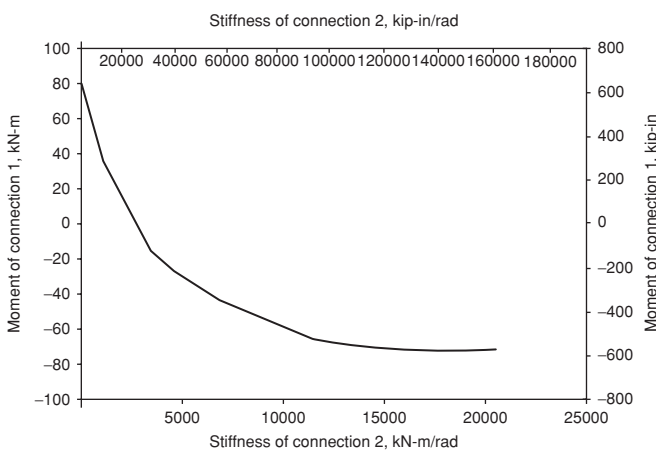


Figure 8. Effect of Connection 2 stiffness on Connection 1 bending moment

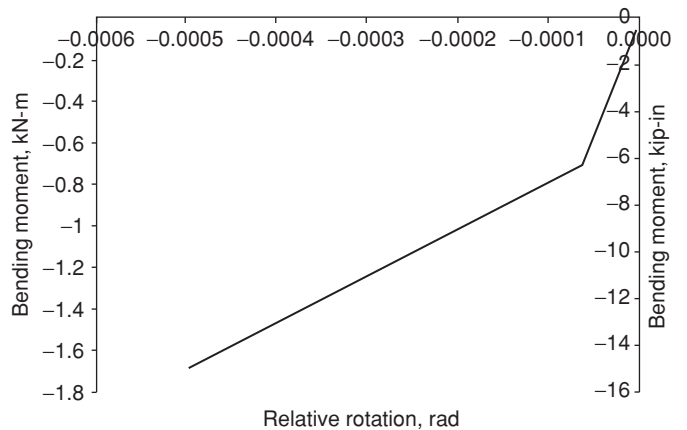


Figure 10. Moment-rotation behavior of Connection 1 for Connection 2 asymptotic stiffness of 2,850 kN-m/rad (25,000 kip-in/rad)

model of Eqn 5 for each of the connection of the aforementioned frame:

Connection 1:

$$R_{ki} = 11,299 \text{ kN-m/rad (100,000 kip-in/rad)}$$

$$R_b = 2,260 \text{ kN-m/rad (20,000 kip-in/rad)}$$

$$\theta_o = 0.00005 \text{ rad}$$

$$n = 50$$

Connection 2:

$$R_{ki} = 11,299 \text{ kN-m/rad (100,000 kip-in/rad)}$$

$$R_b = \text{is varied}$$

$$\theta_o = 0.0002 \text{ rad}$$

$$n = 50$$

The asymptotic stiffness R_b of Connection 2 was then varied between 2,260 (20,000 kip-in/rad) and 3,390 kN-m/rad (30,000 kip-in/rad). As predicted earlier, Figure 9 shows that Connection 1 loads in the same direction with the asymptotic stiffness value of

3,390 kN-m/rad (30,000 kip-in/rad). Figure 10 shows that for the asymptotic stiffness of Connection 2 equal to 2,825 kN-m/rad (25,000 kip-in/rad), Connection 1 continues to load in the same direction. Connection 1 starts to unload when the asymptotic stiffness of Connection 2 drops approximately below the value of 2,768 kN-m/rad (24,500 kip-in/rad) as shown in Figure 11. For values of Connection 2 asymptotic stiffness above 2,768 kN-m/rad (24,500 kip-in/rad), Connection 1 will continue to load in the negative direction. Figures 12 and 13 represent the unloading behavior of Connection 1 due to the values of asymptotic stiffness of Connection 2 equal to 2,757 kN-m/rad (24,400 kip-in/rad) and 2,260 kN-m/rad (20,000 kip-in/rad), respectively. Moreover, Figure 13 shows that the degraded stiffness of Connection 2 has caused Connection 1 to go through a complete unloading and reverse loading without column bifurcation.

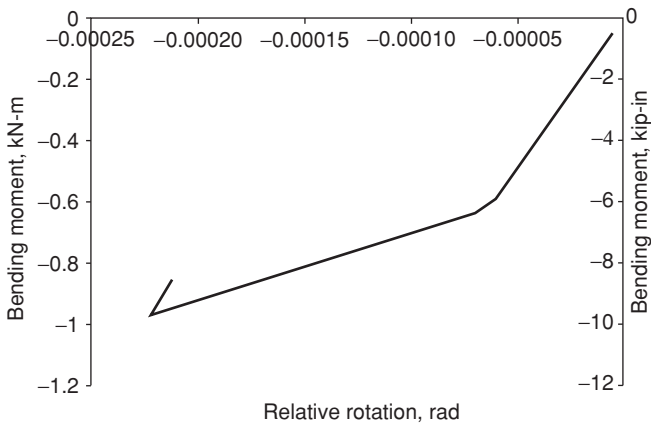


Figure 11. Moment-rotation behavior of Connection 1 for Connection 2 asymptotic stiffness of 2,782 kN-m/rad (24,500 kip-in/rad)

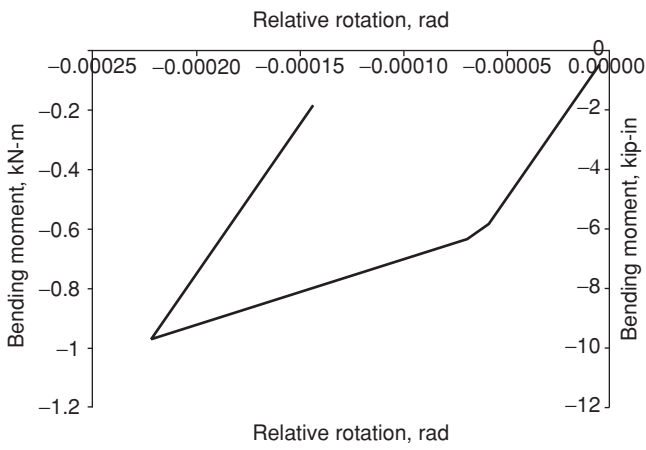


Figure 12. Moment-rotation behavior of Connection 1 for Connection 2 asymptotic stiffness of 2,736 kN-m/rad (24,000 kip-in/rad)

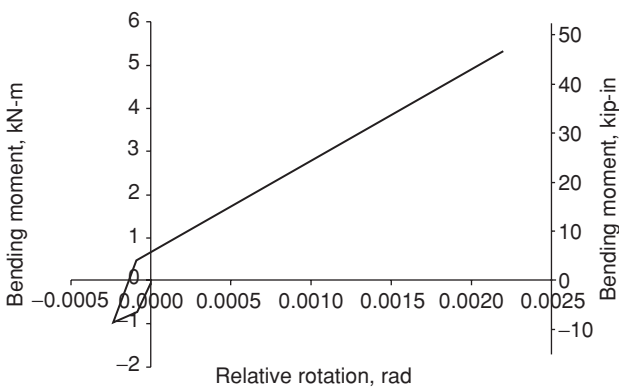


Figure 13. Moment-rotation behavior of Connection 1 for Connection 2 asymptotic stiffness of 2,280 kN-m/rad (20,000 kip-in/rad)

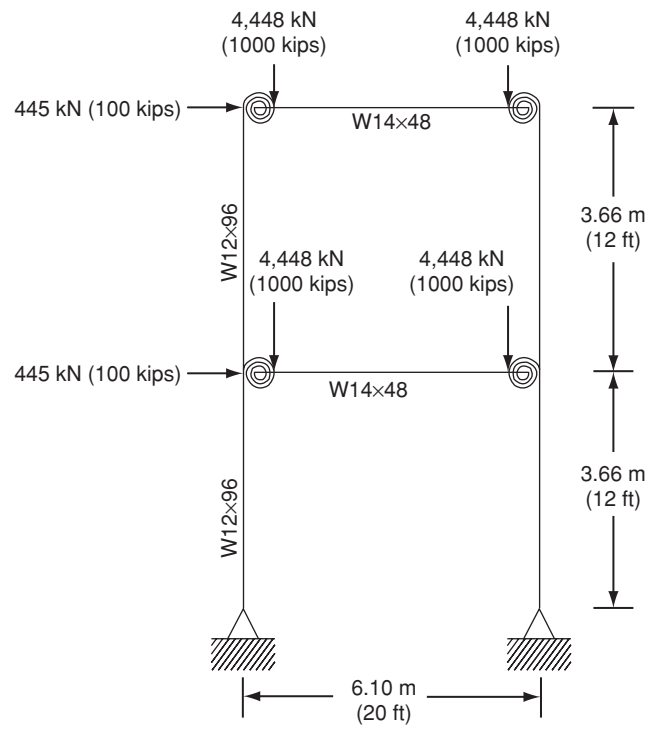


Figure 14. Example frame 1

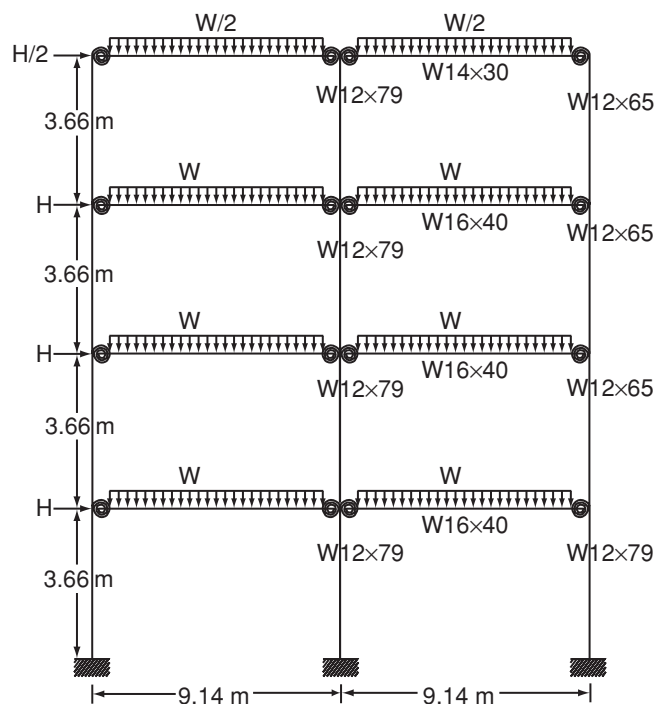


Figure 15. Example frame 2

(Note: $W=26.3$ kN/m (0.15 kip/in) and $H=31$ kN (7 kips))

7. CONCLUSIONS

A semi-rigid frame analysis computer algorithm is developed to consider connection unloading. A kinematic hardening equation to model the pseudo-cyclic behavior of semi-rigid connections is adopted. A unique solution technique that simultaneously iterates to find the incremental connection element and member geometric stiffness of the structure is introduced to solve the nonlinear system equations.

A parametric-type study was conducted on a simple one-story, one-bay frame with two connections in which the stiffness of one of the connections (Connection 1) was kept constant while the stiffness of the other connection (Connection 2) was varied. It was shown that as the stiffness of Connection 2 increases beyond a certain value, Connection 1 undergoes a moment reversal. Furthermore, the post yield stiffness of Connection 2 was varied, and its effect on connection 1 was studied. The analysis results indicated that a decrease in the post yield stiffness of Connection 2 caused moment reversal in Connection 1.

This study, as a proof of concept, shows that different connection properties could cause moment reversal in one or multiple connections. It is noted that in some cases moment reversal can be considered a positive effect since the connection stiffness increases during the unloading phenomenon given the connection is yielded, and its stiffness is the post yield stiffness just before unloading.

8. ACKNOWLEDGEMENTS

The Financial support of the National Science Foundation (Grant EEC-9820102) and the NSF-EPSCoR funds for student support via the University of North Dakota are greatly acknowledged.

REFERENCES

- Abolmaali, A. (1999). *Cyclic Nonlinear Finite Element Dynamic Analysis of Steel Frames With Flexible Joints*, Ph.D. Dissertation submitted as partial fulfillment for degree of Doctor of Philosophy, School of Civil and Environmental Engineering and Environmental Science, University of Oklahoma, Norman, Oklahoma.
- Abolmaali, A., Kukreti, A.R. and Razavi, S.H. (2003). "Cyclic performance of semi-rigid double web angle steel connections", *Journal of Construction Steel Research*. Vol. 59, No. 8, pp. 1057–1082.
- Astaneh, A., Nader, M.N. and Malik, L. (1989). "Cyclic behavior of double web angle connections", *Journal of Structural Engineering*, ASCE, Vol. 115, No. 5, pp. 1101–1118.
- Baker, J.P. (1931). *Methods of Stress Analysis, First and Second Reports*, Steel Structures Research Committee, HMSO, London, England.
- Bhatti, M.A. and Hingtgen, J.D. (1995). "Effects of connection stiffness and plasticity on the service load behavior of unbraced steel frames", *Engineering Journal*, AISC, Vol. 32, No.1, pp. 21–33.
- Chen, W.F., Goto, Y. and Liew, R. (1996). *Stability Design of Semi-Rigid Frames*, John Wiley and Sons, New York.
- Chen, W.F. and Lui, E.M. (1991). *Stability Design of Steel Frames*, CRC Press, Boca Raton.
- Christopher, J.E. and Bjorhovde, R. (1998). "Response characteristics of frames with semi-rigid connections", *Journal of Constructional Steel Research*, Vol. 46, No. 1–3, on CD ROM.
- Gere, J.M. and Weaver, W. (1965). *Analysis of Frame Structures*, Van Nostrand, Princeton NJ.
- Goto, Y. and Chen, W.F. (1987). "On the computer-based design analysis for the flexibly jointed frames", *Journal of Constructional Steel Research*, Vol. 8, Special Issue on Joint Flexibility in Steel Frames, pp. 203–31.
- King, W.S. and Chen, W.F. (1993). "LRFD Analysis for semi-rigid frame design", *Engineering Journal*, AISC, Vol. 30, No. 4, pp. 130–140.
- Kukreti, A.R. and Abolmaali, A. (1999). "Moment-rotation hysteresis behavior of top and seat angle steel frame connections", *Journal of Structural Engineering*, Vol. 125, No. 8, pp. 810–820.
- Kukreti, A.R. and Abolmaali, A. (2000). "Dynamic analysis of steel frames with semi-rigid connections", *Proceedings of the XIXII Southeastern Conference on Theoretical and Applied Mechanics*, Deerfield Beach, Florida, May, pp. 13–16.
- Li, T.Q., Choo, B.S. and Nethercot, D.A. (1995). "Connection element method for the analysis of semi-rigid frames", *Journal of Constructional Steel Research*, Vol. 32, No. 2, pp. 143–171.
- Lightfoot, E. and Le Messurier, A.P. (1974). "Elastic analysis of frameworks with elastic connections", *Journal of Structural Division*, ASCE, Vol. 89, No. ST6, pp. 1297–309.
- Lionberger, S.R. and Weaver, W.Jr. (1969). "Dynamic response of frames with non-rigid connections", *Journal of the Engineering Mechanics Division*, ASCE, Vol. 95, No. EMI, Proc. Paper 6393, pp. 95–114.
- Livesley, R.K. (1964). *Matrix Methods of Structural Analysis*, 1st edn. Pergamon Press, Oxford.
- Lui, E.M. and Chen, W.F. (1987). "Steel frame analysis with flexible joints", *Journal of Constructional Steel Research*, Vol. 8, pp. 161–202.
- Monforton, G.R. and Wu, T.S. (1963). "Matrix analysis of semi-rigidly connected frames", *Journal of the Structural Division*, ASCE, Vol. 89, No. ST6, pp. 13–42.
- Nethercot, D.A. (1986). "The behaviour of steel frame structures allowing for semi-rigid joint action", *In Steel Structures; Recent Research Advances and their Application to Design*, Pavlovic, M.N. ed., Elsevier Applied Science Publishers, pp.135–152.
- Poggi, C. (1988). "A finite element model for the analysis of flexibly connected steel frames", *International Journal for Numerical Methods in Engineering*, Vol. 26, pp. 2239–2254.

- Popov, E.P. and Bertero, P. (1973). "Cyclic loading of steel beams and connections", *Journal of the Structural Division*, ASCE, Vol. 99, No. ST6, pp. 1189–1204.
- Rathbun, J.C. (1936). "Elastic properties of riveted connection", *Transactions*, ASCE, No. 101 pp. 524–63.
- Rodrigues, F.C., Saldanha, A.C. and Pfeil, M.S. (1998). "Non-linear analysis of steel frames with semi-rigid connections", *Journal of Constructional Steel Research*, Vol. 46, No. 1-3, pp. 94–97.
- Sack, L.R. (1994). *Matrix Structural Analysis*, Waveland Press Inc., Illinois.
- Suko, M. and Adams, P.F. (1971). "Dynamic analysis of multibay multistory frames", *Journal of the Structural Division*, ASCE, Vol. 97, No. ST10, pp. 2519–33.
- Tsai, K.C., Wu, S.W. and Popov, E.G. (1995). "Experimental performance of seismic steel beam-column moment joints", *Journal of Structural Engineering*, Vol. 121, No. 6, pp. 925–931.

Copyright of *Advances in Structural Engineering* is the property of Multi-Science Publishing Co Ltd and its content may not be copied or emailed to multiple sites or posted to a listserv without the copyright holder's express written permission. However, users may print, download, or email articles for individual use.